Appl. Phys. A (2017) 123:490
DOI 10.1007/s00339-017-1105-0

Applied Physics A
Materials Science & Processing

Laser-assisted fabrication and size distribution modification of colloidal gold nanostructures by nanosecond laser ablation in different liquids

R. G. Nikov[1] · N. N. Nedyalkov[1] · P. A. Atanasov[1] · D. B. Karashanova[2]

Received: 13 April 2017 / Accepted: 22 June 2017 / Published online: 29 June 2017

Abstract This study presents results on pulsed laser ablation of gold target immersed in different liquids. In the experiments chloroform, toluene and ethanol are used as liquid media for the laser ablation. Two different wavelengths: the fundamental (1064 nm) and second harmonic (532 nm) of a Nd:YAG laser, are utilized to produce various colloids. The optical properties of the colloids were evaluated by optical transmittance measurements in the UV–Vis spectral range. The morphology of the colloidal nanoparticles created and the evaluation of their size distribution are investigated by transmission electron microscopy. The selected area electron diffraction is employed for chemical phase identification of the created nanostructures. Ablation in chloroform resulted in formation of spherical and spheroidal gold nanoparticles with the similar mean size at both laser wavelengths used—11.5 nm at 1064 and 9.3 nm at 532 nm. Nanoparticles with smaller mean size (below 5 nm) in the case of ablation in toluene were observed. Spherical nanoparticles with mean diameter of 7.7 nm produced by 1064 nm and thin elongated nanostructures with thickness of about 5 nm using 532 nm are observed in the case of ablation in ethanol. An additional laser irradiation of the colloids demonstrated the changing of the optical properties and size distribution of the nanostructures produced by ablation in ethanol and chloroform. The irradiation of toluene-based colloid does not induce observable change of the colloid properties.

1 Introduction

Gold (Au) nanoparticles (NPs) attract an extensive attention in various fields of physics, chemistry, medicine, material science, and photonics, due to their unique physical and chemical properties [1–6]. Extraordinary electronic, magnetic, and catalytic properties of the NPs are due to their high surface area to volume ratio [7]. One of the most attractive properties of noble metal NPs is related to the efficient excitation of collective electron oscillations, i.e. surface plasmon resonance (SPR). The plasmon characteristics of these metal NPs vary with their size, shape, surface chemistry, and crystallinity or aggregation state [8–10], which enables tuning of their optical and electronic properties.

Au NPs have optical, electrical, magnetic, and mechanical properties, which make them suitable for many applications such as drug and gene delivery [11, 12], the ability to generate table immobilization of biomolecules [13], and in several targeting applications [14]. Au nanostructures possess the ability to produce heat after absorbing light, which provides a medicinal usage named as photothermal therapy [15, 16]. The strong enhancement of the electromagnetic field near the Au-containing nanostructures as a result of excitation by laser radiation has been successfully employed to enhance Raman signals in surface-enhanced Raman spectroscopy (SERS) applications [17, 18] for the detection of proteins, pollutants, and other molecules. Colloidal Au NPs have been designed for use as conductors from printable inks to electronic chips [19]. In these applications nanoscale Au particles are used

✉ R. G. Nikov
rosen_nikov@abv.bg

[1] Institute of Electronics, Bulgarian Academy of Sciences, Tzarigradsko Chaussee 72, 1784 Sofia, Bulgaria

[2] Institute of Optical Materials and Technologies, Bulgarian Academy of Sciences, G. Bonchev Street, Building 109, 1113 Sofia, Bulgaria

to connect resistors, conductors, and other elements of an electronic chip. Au NPs are also utilized as catalysts in various chemical reactions [20].

A number of methods, such as chemical reduction [21], photochemical [22], electrochemical [23], and biosynthesis [24], can be used for producing colloidal Au NPs. In the past decade, a method known as pulsed laser ablation of solid target in liquid environments has emerged as one of the most promising techniques to obtain nanostructured materials in liquid medium [25–27]. The laser ablation is relatively simple, cheap, effective, and environmental friendly method, which stands out for its fast and direct implementation that does not involve several steps or long processing times. The control of parameters such as laser wavelength, pulse energy, repetition rate, number of pulses, and liquid environments allows the fabrication of colloidal NPs with specific characteristics (morphology, size distribution, shape, composition and structure) making them suitable for various applications.

In the majority of studies, the laser ablation in liquid is performed in aqueous solutions [28–30]. Although there are works on laser ablation in organic liquids for fabrication of colloids [31–36], there are insufficient data about the influence of the various processing parameters as wavelength for example on the characteristics of the nanostructures produced by this method. Furthermore, there are controversial data about optical properties of such colloids and how the plasmon resonance behavior is influenced [34, 36]. Study of the preparation of colloidal Au NPs by laser ablation in organic solvents is very important from the viewpoint of obtaining NPs in solvents, which can also solubilize organic molecules useful for functionalizing Au NPs [37].

In the present study, the colloidal Au NPs are prepared by laser ablation of a Au target in three different liquids—chloroform, toluene, and ethanol. These liquids are the basis for preparing colloidal inks used in the printed and organic electronics for printing of conductive circuits [38] and active layers of organic photovoltaics [39]. The influence of laser wavelength, on structure, morphology, size distribution, shape, and optical properties of the obtained nanostructures is studied by means of transmission electron microscopy (TEM), selected area electron diffraction (SAED), and UV–Vis absorption measurements. Additional laser irradiation of the as prepared colloids is performed in order to demonstrate possibility of changing their optical properties and eventually narrowing the particles size distribution. The presented method could be an alternative of the conventional chemical methods for synthesis of colloidal inks. Printing of these nanoparticle-based inks on appropriate surfaces by conventional printer can provide easy and efficient method for the preparation of SERS substrates.

2 Experimental

Ablation of Au target (purity 99.99%) in liquids is obtained using the fundamental wavelength (1064 nm) and second harmonic (532 nm) radiation from a Q-switched Nd:YAG laser system (pulse duration $\sim$17 ns) operating with a repetition rate of 10 Hz. The laser beam is focused on the Au surface using a fused silica lens. The Au target is placed on the bottom of a glass vessel filled with the solvent liquid (chloroform, toluene, or ethanol) and the liquid level above the target surface is 5 mm. In all experiments, the duration of ablation process is 6 min and the scanning of the target surface is carried out by means of a XY translation stage. The laser fluence is chosen to be about three times above the threshold fluence for each laser wavelength. Thus, the laser fluence is 12 J/cm^2 at fundamental wavelength and 6 J/cm^2 using second harmonic for all liquids used. A series of experiments on irradiation of Au target with different laser fluences are conducted in order to determine the threshold fluence. The fluence at which the target surface modification appears after single shot, observed by optical microscope, is defined as the threshold one.

Immediately after preparation of the colloids, additional laser irradiation is performed. In order to ensure more efficient irradiation process the colloidal solution is poured in a narrow container (glass cuvette) and the irradiation is carried out with an unfocussed laser beam. Thus, the irradiation of large part of the volume of the colloid is obtained. The diameter of the laser spot on the liquid surface is about 6 mm and the height of the liquid in the cuvette is 2.5 cm. The second harmonic (532 nm) of the Nd:YAG laser is chosen for irradiation, because it lies inside the SPR band of the Au NPs. The laser pulse energy used for irradiation is of 60 mJ. The reason for choosing this laser energy is that the continuing exposure at higher energy leads to modification of the bottom of the vessel containing the colloid. On the other hand, the use of lower laser energy also leads to changes in the optical properties of the colloid, but the process is slower.

The colloids produced by laser ablation and irradiated colloids are immediately characterized by absorbance spectra recorded by an UV–Visible spectrometer (Ocean Optics HR 4000) in the range of 300–900 nm. A transmission electron microscope JEOL JEM 2100 at accelerating voltage of 200 kV is employed to visualize the obtained NPs. The TEM samples are prepared by adding droplets of the colloidal solution of interest on carbon-coated copper grids and allowing them to dry in air. For identification of the phase composition of the NPs produced, SAED is performed. The EMCAT/EMFIT computer program [40] is used to interpret the SAED patterns and to identify the composition of the samples.

3 Results and discussion

3.1 Laser ablation in chloroform

Colloidal solutions produced by laser ablation of a gold target in chloroform ($CHCl_3$) have a pale pink color. The optical absorption spectra of the colloids are measured immediately after their preparation. A comparison of the absorbance spectra of the colloids obtained using the fundamental laser wavelength and second harmonic and the spectrum of pure chloroform is shown in Fig. 1a. A surface plasmon resonance (SPR) band in the range of 500 and 600 nm, characteristic of the presence of nanosize Au particles, is observed in the spectra of colloids fabricated at both wavelengths. It should be mentioned that other authors did not observe plasmon band in the optical spectra of the colloids obtained by laser ablation of a gold target in chloroform [34]. The chemical state of the ablated particles has been investigated by means of X-ray photoelectron spectroscopy (XPS) analysis suggesting the presence of gold–chlorine compounds in the colloid. One possible reason for the different composition of the colloidal NPs could be attributed to the relatively low laser fluence (between 0.2 and 1 J/cm^2) used by them compared to the laser fluence used in our ablation experiments (6–12 J/cm^2). The higher laser fluence may result in significant rise of the temperature of the already formed particles due to absorption of the laser radiation and decomposition of the gold–chlorine phase that is unstable at high temperature.

The slight red-shift and higher intensity of the SPR maximum in the spectrum of the colloid fabricated at wavelength of 1064, compared to that produced at 532 nm, could be attributed to a larger mean size of the NPs in the first case [9]. In order to confirm the above statement and to study more carefully the shape and size distribution of the produced particles, drops of the colloids are deposited onto a carbon-coated copper grid for TEM analysis. In Fig. 2a, b, TEM images of the NPs produced by laser ablation of a gold target in $CHCl_3$ by using laser irradiation at wavelength of 1064 nm (a) and 532 nm (b), and the histograms of the particles size distribution, are presented. The corresponding SAED patterns are also displayed below the TEM images. The diffraction rings in the both SAED patterns shown in Fig. 2a, b can be assigned to the (111), (200), (220), (311), and (331) crystal planes of the cubic gold with lattice parameters $a = 4.0786$ Å, PDF 04-0784. Observing the TEM images in Fig. 2a, b, we can infer that the predominant shape of the particles is spherical or spheroidal. However, it should be noted that the larger particles have an asymmetrical or elongated shape, which is probably due to aggregation of smaller particles in a later stage, after the condensation of the plasma plume. Numerical

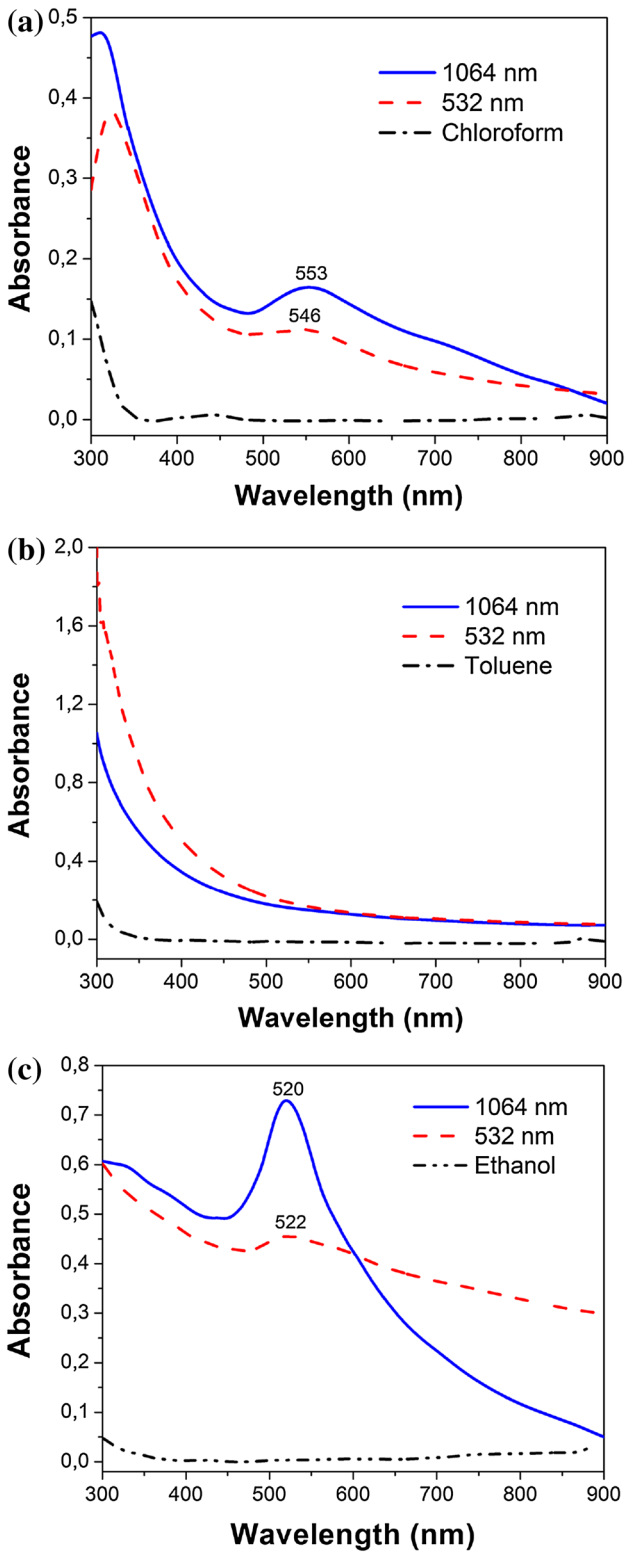

Fig. 1 Optical absorption spectra of colloids produced by laser ablation at wavelengths of 1064 and 532 nm of gold target in different liquids: chloroform (**a**), toluene (**b**) and ethanol (**c**). The absorption spectra of pure liquids are also presented

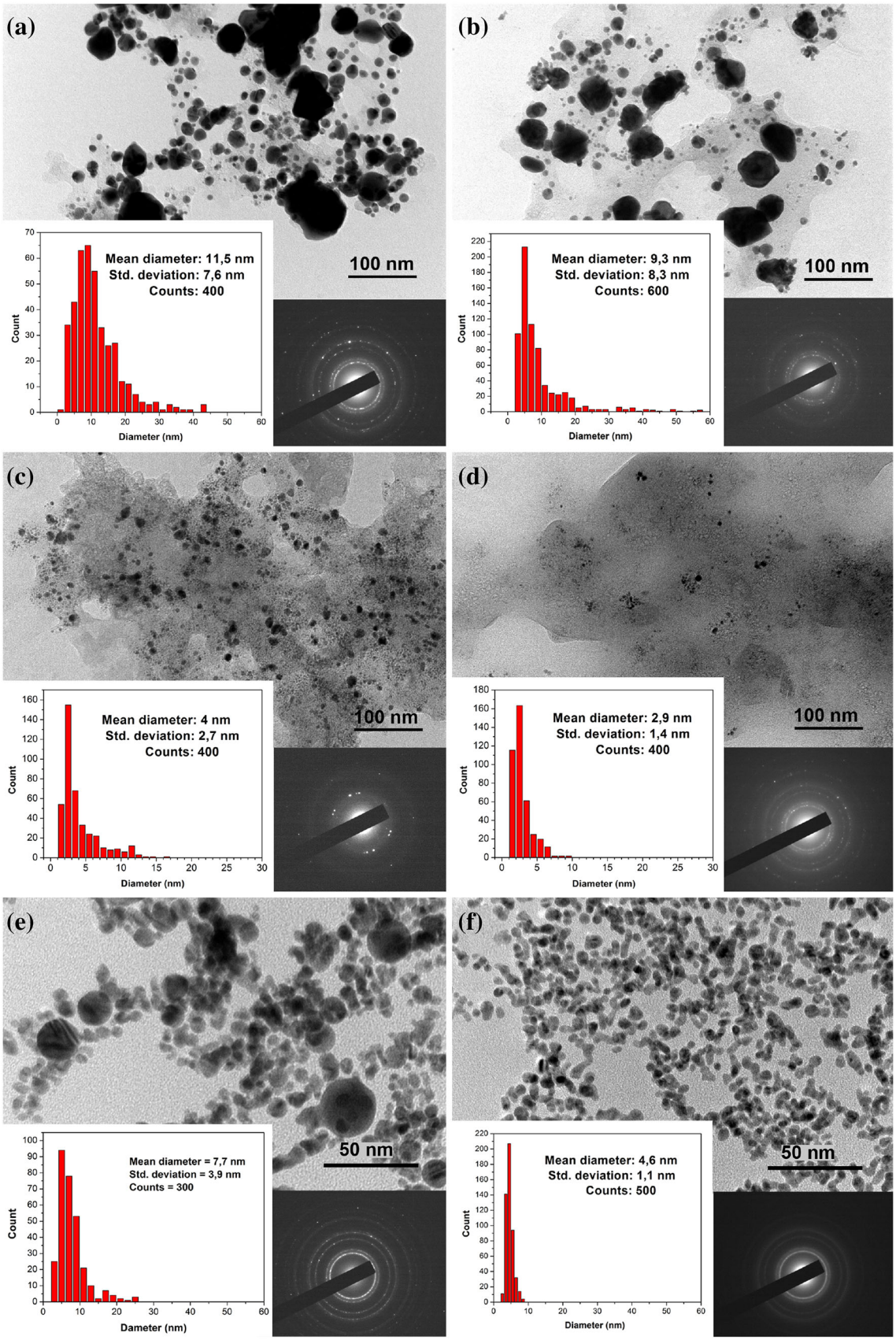
(a)
Mean diameter: 11,5 nm
Std. deviation: 7,6 nm
Counts: 400
Count
Diameter (nm)
100 nm
(b)
Mean diameter: 9,3 nm
Std. deviation: 8,3 nm
Counts: 600
Count
Diameter (nm)
100 nm
(c)
Mean diameter: 4 nm
Std. deviation: 2,7 nm
Counts: 400
Count
Diameter (nm)
100 nm
(d)
Mean diameter: 2,9 nm
Std. deviation: 1,4 nm
Counts: 400
Count
Diameter (nm)
100 nm
(e)
Mean diameter = 7,7 nm
Std. deviation = 3,9 nm
Counts = 300
Count
Dameter (nm)
50 nm
(f)
Mean diameter: 4,6 nm
Std. deviation: 1,1 nm
Counts: 500
Count
Diameter (nm)
50 nm

◀**Fig. 2** TEM images of Au NPs produced by laser ablation at 1064 and 532 nm of gold target in three different liquids: chloroform using 1064 nm (**a**) and 532 nm (**b**); toluene 1064 nm (**c**) and 532 nm (**d**); ethanol 1064 nm (**e**) and 532 nm (**f**). The corresponding histograms of the particle size distribution are also presented and their numerical characteristics are given. Below the TEM images are shown corresponding SAED patterns

characteristics of the histograms reveal a slight increase in the mean particle size (from 9.3 to 11.5 nm) with increasing the laser wavelength. On the other hand, the standard deviation slightly decreased with increasing the laser wavelength (from 8.3 to 7.6 nm). The larger mean size of the particles obtained using radiation at 1064 nm explains the red-shift of their SPR band (Fig. 1a) compared to that of the NPs produced by ablation at 532 nm.

The TEM images shown in Fig. 2a, b also indicated the presence of a paler gray shell around the NPs. It is reported that the laser ablation of metals in organic solvents can produce pyrolysis of organic molecules with subsequent covering of the particle surface by carbon shell [35]. Thus, forming a carbon shell or matrix could limit the further growth of the particles and may cause a suppression of the plasmon properties of the metal NPs. Using the Mie model, Amendola et al. [35] have shown that increasing the thickness of the graphite shell around a spherical Au nanoparticle leads to attenuation of the SPR band. In fact, the plasmon resonance intensity will depend on the ratio between the particle size and the shell thickness. As the particle size in the case of using laser ablation at 1064 nm is higher, the effect of shell plasmon quenching will be less expressed resulting in stronger SPR peak.

3.2 Laser ablation in toluene

Laser ablation of a gold target in toluene (C_7H_8) resulted in formation of colloidal solutions that have yellowish amber color instead of pink reddish, typical for the Au NPs. It should be mentioned that after a several minutes the ablation is strongly reduced at both laser wavelengths used. This effect probably is due to the scattering and absorption of the laser radiation by already formed nanostructures in the liquid. In Fig. 1b are presented the UV–Vis spectra of the colloids produced by laser ablation in toluene using wavelengths of 1064 and 532 nm, where one can note the absence of the SPR band. Despite the absence of the plasmon band a significant increase in the absorbance in the range of 300–500 nm in the spectra of both colloids compared to that of pure toluene is observed. This effect hints change of the liquid composition induced by the laser treatment.

For visualization of the shape of the nanostructures obtained, assessment of their size distribution and identification of their phase composition, TEM and SAED analysis of the dried colloids are performed and the results are shown in Fig. 2c, d. Here, similarly to the ablation in chloroform, the diffraction rings and spots in SAED patterns of both laser wavelengths used can be assigned to the (111), (200), (220), (311), and (331) crystal planes of the gold (Au cubic, lattice parameters $a = 4.0786$ Å, PDF 04-0784). The TEM images and histograms of the particle size distribution of NPs produced by using fundamental wavelength and second harmonic are shown in Fig. 2c, d, respectively. Relatively small NPs in both TEM images are observed. On the basis on the histograms presented in Fig. 2c, d may be defined an increase of the mean particle size (from 2.9 to 4 nm) and standard deviation (from 1.4 to 2.7 nm) with the increase of the laser wavelength. One of the reasons for the formation of small particles in the case of ablation in toluene could be the presence of dense material around the particles, which is observed in both TEM images. Similar shell or matrix around the nanoparticle was observed in the considered earlier case of ablation in chloroform. The origin of this shell has already been discussed, namely the occurrence of the pyrolysis process leading to the decomposition of the organic molecules of the liquid and subsequent covering of the surface of gold particles with graphite or carbon shell [35]. However, the carbon matrix, appearing as a dark gray background around the particles in Fig. 2c, d is more solid and thicker compared to that observed in the case of ablation in chloroform (Fig. 2a, b), which explains the smaller mean particle size in the case of ablation in toluene. Consequently, this dense carbon shell stops coalescence and growth of Au NPs in the early stage, when the mean particle size is few nanometers. Moreover, the presence of thick carbon shell around the gold particles is also responsible for the suppression of the SPR band in the optical absorption spectra of the colloids displayed in Fig. 1b. It has been reported that by oxidizing the carbon matrix it is possible to recover the SPR band of colloids prepared by laser ablation of gold in toluene [35]. On the other hand, composite structures based on graphite and gold NPs can be used for sensor applications [41], making the laser ablation a simple and effective method for fabricating such type of material.

The main reason for the formation of different shell around the NPs in the case of ablation in toluene and chloroform probably is rooted in the different reactivity of both solvents. After the plasma plume expands and cools in the liquid, the temperature of the solution reaches that of the plasma plume, i.e. 10^3 K, with consequent degradation, ionization, and pyrolysis of solution molecules. It could be expected that pyrolysis of the solvent is realized at different thermo physical parameters depending on the type. Moreover, different solvents generate different byproducts with specific chemical and physical properties during laser

ablation, which complicates determination of all these byproducts [27]. Therefore, further research is needed to clarify the process of pyrolysis during laser ablation in the presence of organic compounds and the role of pyrolysis byproducts on the nucleation and growth processes of the NPs.

3.3 Laser ablation in ethanol

An intensive ablation of the Au target in ethanol (C_2H_6O) at both laser wavelengths used is observed. In turn, this leads to intense coloration of the colloids, as their colors are pink and ink blue using 1064 and 532 nm, respectively. The optical absorption spectra of the colloids prepared by laser wavelengths of 1064 and 532 nm are presented in Fig. 1c. A clearly expressed SPR band with a maximum at 520 nm can be seen in the case of ablation by the fundamental laser wavelength. The presence of a single peak and its position in the spectrum indicate the presence of Au spherical particles with diameter below 60 nm [9]. In the optical spectrum of the colloid prepared by the 532-nm laser wavelength, the SPR band is less pronounced than that in the case of ablation with 1064 nm.

In order to assess the shape and size distribution of the obtained nanostructures, TEM analysis is performed. TEM micrographs and corresponding histograms of the size distribution of the nanostructures produced by laser ablation at both 1064 and 532 nm laser wavelengths are shown in Fig. 2e, f. The SAED analyses of the obtained nanostructures are presented below both the TEM images. Phase identification reveals the presence of cubic gold with lattice parameter $a = 4.0786$ Å (PDF 04-0784). The TEM images express different nanostructures in terms of shape and size for both the cases. Formation of separated spherical and spheroidal shaped NPs with relatively wide size distribution is observed when the fundamental laser wavelength is used (Fig. 2e). The histogram of the particle size distribution reveals mean particle diameter of 7.7 nm and standard deviation of 3.9 nm. In the case of ablation by 532 nm thin nanostructures (chain-like shape) of approximately equal thickness are observed (Fig. 2f). The mean size of the particles forming the nanostructures is 4.6 nm and the standard deviation is 1.1 nm. These elongated nanostructures are probably formed because of joining of already created particles in the colloid. The wavelength of the second harmonic of the used laser, in contrast to the fundamental wavelength, is situated in the SPR band of the Au NPs. Thus, the absorption of laser radiation from the NPs may lead to fragmentation of the larger NPs and partial melting of the surface of the smaller particles, where the melting temperature is significantly lower than that of the bulk material [42]. Namely, the fragmentation of the larger particles and merging of smaller ones are the reason for the production of uniform in shape and size nanostructures as shown in Fig. 2f [43]. It is notable that chain-assembled NPs are also observed in the case of ablation by 1064 nm, but only for the smallest particles (Fig. 2e). The formation of nanoparticle chains in the case of laser ablation in ethanol can be explained by asymmetric distribution of charge on the surface of NPs, which causes dipole–dipole interaction and can lead to linear aggregation [44].

The TEM images also reveal an absence of the background materials as seen in the case of ablation in chloroform and toluene. It can be attributed to the fact that the decomposition of the ethanol leads to formation of alcoholates instead of carbon compounds [27]. This may be the reason for formation of NPs without cover and, respectively, clearly expressed SPR band.

Generally, the Au nanostructures obtained by laser ablation in chloroform, toluene, and ethanol exhibit lower stability over time compared to Au nanostructures in water [27]. It should be mentioned that after 1 week of storage (at room temperature) of the colloids produced by ablation in chloroform and toluene, large microparticles are observed due to the process of aggregation and precipitation of the components in the colloids. The lower stability of Au NPs obtained in these organic solvents can be the combined effect of the lower dielectric constant, compared to water, and of the lower *Z*-potential of NPs, due to adsorption of solvent pyrolysis byproducts on their surface [45]. Our observation indicates that the Au NPs in ethanol have higher stability than NPs in toluene and chloroform. There is not observed (with the naked eye) large microparticles or sedimentation within 1 month after the colloid preparation. However, some change in the colloid color is observed which is most likely due to partial aggregation of the Au NPs. It is reported that the greater stability over time of the NPs obtained in ethanol, compared to other organic solvents, may be explained by surface complexation with alcoholates, which are negatively charged molecules [46, 47].

3.4 Laser irradiation of the fabricated colloids

In this section, we will consider the influence of the additional laser irradiation on the characteristics of the already prepared colloids. The three different colloids produced by ablation of gold target in chloroform, toluene, and ethanol using laser wavelength of 1064 nm were exposed to laser irradiation. This wavelength ensures the highest efficiency of fabrication in terms of particle density. However, the size distribution is rather broad as it can be seen in Fig. 2a, e. Here we should mention that the changes occurring in the colloids as a result of the continuous increase of the duration of irradiation were investigated by direct measurement of their optical spectra. On

the base of these measurements, it was found that in the case of irradiation at wavelength of 532 nm of the colloid, created by ablation in toluene, no significant change of its absorbance spectrum is realized. As in the case of as prepared colloids, SPR band is not observed in the spectrum of the irradiated colloid. For this reason, the colloid is also irradiated with the laser wavelength of 355 nm where the absorbance of the colloid is significant. However, the result does not differ greatly from that obtained in the case of irradiation with the second harmonic. Therefore, in this section will be discussed in detail only the cases of laser irradiation of colloids synthesized by ablation in ethanol and chloroform.

The evolution of the absorbance spectrum of the colloids produced by ablation in ethanol and chloroform as a result of the continuous increase of the duration of irradiation is presented in Fig. 3. First, we will consider the case of laser irradiation of the colloid created by ablation in ethanol (Fig. 3a). After the first 5 min of irradiation is observed a significant decrease in the absorbance of the colloid in the range of 550–900 nm, whereas the rest of the spectrum (300–550 nm) containing the SPR band is practically unchanged. The main reason for this behavior is probably fragmentation of the largest particles in the solution due to absorption of laser radiation. After another 5 min of irradiation (total 10 min), a further narrowing of the right side of the SPR band from its center (around 520 nm) to approximately 700 nm was observed. In the range after 700 nm absorption spectrum remains unchanged. The latter result can be explained by the fact that after the first 5 min of irradiation fragmentation leads to the disappearance of the largest particles in the solution while after the 10 min occurs further fragmentation of the particles. It can be seen (Fig. 3a) that after an additional 5 min of irradiation (total 15 min), there was no change in the absorption spectrum of the colloid which is an indication of a saturation of the fragmentation process.

In order to confirm the above statements TEM analysis of the colloid before and after irradiation has been made. TEM micrograph of the nanostructures obtained after ablation with 1064 nm of gold target in ethanol without additional laser irradiation was already shown in Fig. 2e. In Fig. 4a are presented a TEM image and the corresponding histogram of the size distribution of the NPs obtained after 10 min laser irradiation by wavelength of 532 nm and pulse energy of 60 mJ. It is clearly seen that as a result of the laser irradiation spherical NPs with an approximately uniform size (mean diameter = 9.5 nm) are formed (Fig. 4a). Comparing the histograms of Fig. 2e (before radiation) and Fig. 4a (after irradiation) it can be concluded that as a result of irradiation the portion of particles larger than 15 nm is greatly reduced. Decreasing of the standard deviation from 3.9 to 2.8 nm as a result of irradiation confirms the narrowing of particle size distribution implied by narrowing of the SPR band in the spectra of Fig. 3a.

In the case of irradiation of the colloid produced by ablation in chloroform the evolution of the absorbance spectrum is quite different (Fig. 3b). Narrowing of the SPR band is not observed despite that laser irradiation is performed under the same processing conditions ($\lambda = 532$ nm and $E_{\text{pulse}} = 60$ mJ). Instead, reduction of the absorbance in entire analyzed spectral range accompanied by a blue shift of the SPR maximum is observed. The significant blue shift of the plasmon band from 553 to 526 nm after 5 min of irradiation is primarily due to reduction in the particle size as a result of the fragmentation of the larger particles in the solution caused by absorption of the laser radiation. For confirmation of this assumption, TEM analysis of the

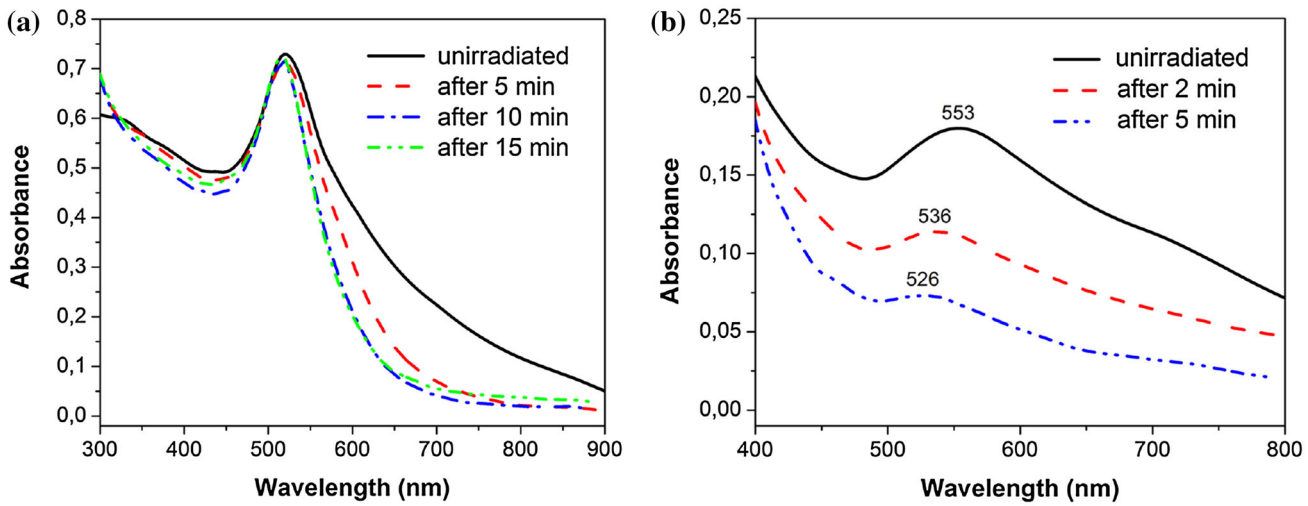

Fig. 3 Evolution of the optical absorption spectra of two different Au colloids during the process of laser irradiation. Both Au colloids are initially produced by laser ablation of gold in different liquid media: **a** ethanol and **b** chloroform

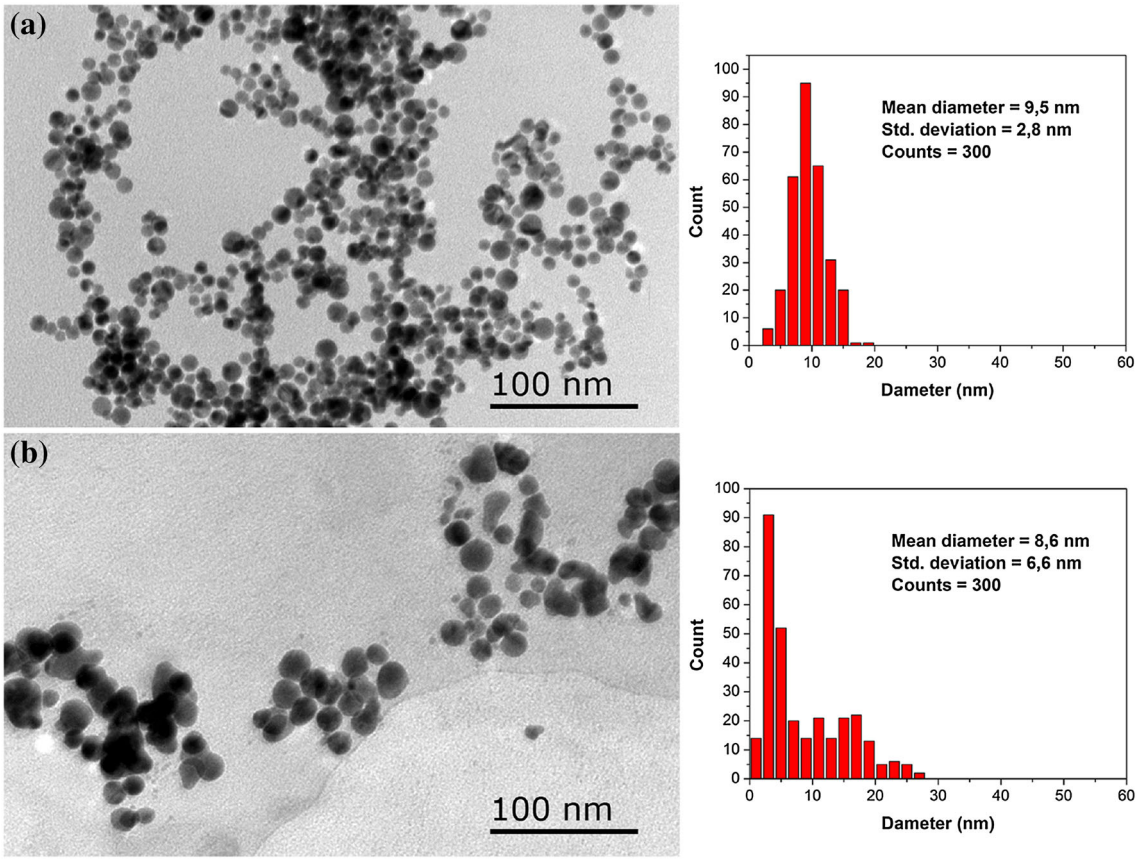

Fig. 4 TEM images of Au NPs produced after laser irradiation by 532 nm and pulse energy of 60 mJ of colloids, initially prepared by laser ablation of gold target in different liquid media: **a** ethanol and **b** chloroform

NPs in the colloid irradiated for 5 min is performed (Fig. 4b). Observing TEM images of the NPs before irradiation (Fig. 2), and after irradiation (Fig. 4b), and comparing their respective histograms, it can clearly be noticed that after the laser irradiation the particles larger than 30 nm completely disappear. Because of fragmentation of larger particles, the mean particle size decreased to 8.6 nm and the standard deviation is reduced to 6.6 nm. The dynamics in the case of modification of colloid properties by laser irradiation is still not clear. One should consider also the presence of different components produced in the ablation process and their role in the NPs size modification. They may also include additional chemical reaction during the post fabrication treatment.

4 Conclusion

In this study we have demonstrated the possibility of obtaining Au NPs by laser ablation in three different liquids—chloroform, toluene, and ethanol. A slight increase in the mean particle size (from 9.3 to 11.5 nm) with increasing the laser wavelength in the case of ablation in chloroform is observed. In the case of ablation in toluene relatively small particles with mean size of 2.9 and 4 nm at laser wavelength of 532 and 1064 nm, respectively, are obtained. The laser ablation of Au target in ethanol using 1064 nm resulted in formation of spherical and spheroidal NPs with diameter of 7.7 nm while the ablation by 532 nm leads to appearance of uniform elongated nanostructures with a mean thickness of 4.6 nm. A single well-defined SPR band in the optical absorption spectra of the colloids produced by laser ablation in chloroform and ethanol is observed in contrast to the case of ablation in toluene. We suppose that the absence of plasmon behavior of the Au particles in toluene is due to the formation of carbon matrix around the NPs in the colloid. The phase identification of the SAED patterns of the samples produced by laser ablation in chloroform, toluene and ethanol demonstrates the presence of cubic gold. The additional laser irradiation of the colloids produced by ablation in ethanol and chloroform leads to a change in their optical properties and to the modification of the size distribution of the NPs in the solutions. The presented results indicate the ability of the method of laser ablation in liquid as a tool for fabrication of complex nanosystems whose characteristics can be

controlled by the processing parameters. The precise tuning of material characteristics would require understanding of the complex physical mechanisms that play a role during the ablation process and formation and dynamics of the NPs.

Acknowledgements The authors acknowledge the financial support of the project DFNP-185 "Preparation of colloids by laser ablation in liquids for printing of two-dimensional and three-dimensional structures" under scientific program "Assistance for young scientists", BAS.

References

1. M.C. Daniel, D. Astruc, Gold nanoparticles: assembly, supramolecular chemistry, quantum-size-related properties, and applications toward biology, catalysis, and nanotechnology. Chem. Rev. **104**, 293–346 (2004)
2. S.J. Guo, E.K. Wang, Synthesis and electrochemical applications of gold nanoparticles. Anal. Chim. Acta **598**, 181–192 (2007)
3. E. Boisselier, D. Astruc, Gold nanoparticles in nanomedicine: preparations, imaging, diagnostics, therapies and toxicity. Chem. Soc. Rev. **38**, 1759–1782 (2009)
4. S.H. Radwan, H.M.E. Azzazy, Gold nanoparticles for molecular diagnostics. Exp. Rev. Mol. Diagn. **9**, 511–524 (2009)
5. W.R. Algar, M. Massey, U.J. Krull, The application of quantum dots, gold nanoparticles and molecular switches to optical nucleic-acid diagnostics. Trends Anal. Chem. **28**, 292–306 (2009)
6. W.E. Bawarski, E. Chidlowsky, D.J. Bharali, S.A. Mousa, Emerging nano-pharmaceuticals. Nanomed. Nanotechnol. Biol. Med. **4**, 273–282 (2008)
7. V.V. Mody, R. Siwale, A. Singh, H.R. Mody, Introduction to metallic nanoparticles. J. Pharm. Bioallied Sci. **2**, 282–289 (2010)
8. C.F. Bohren, D.F. Hufman, *Absorption and scattering of light by small particles* (Wiley, New York, 1983)
9. U. Kreibig, M. Vollmer, *Optical properties of metal clusters* (Springer, Berlin, 1995)
10. M.H. Abdellatif, S. Ghosh, I. Liakos, A. Scarpellini, S. Marras, A. Diaspro, M. Salerno, Effect of nanoscale size and medium on metal work function in oleylamine-capped gold nanocrystals. J. Phys. Chem. Solids **89**, 7–14 (2016)
11. D. Pissuwan, T. Niidome, M.B. Cortie, The forth-coming applications of gold nanoparticles in drug and gene delivery systems. J. Control. Release **149**, 65–71 (2011)
12. P. Ghosh, G. Han, M. De, C.K. Kim, V.M. Rotello, Gold nanoparticles in delivery applications. Adv. Drug Deliv. Rev. **60**, 1307–1315 (2008)
13. D.T. Nguyen, D.-J. Kim, K.-S. Kim, Controlled synthesis and biomolecular probe application of gold nanoparticles. Micron **42**, 207–227 (2011)
14. A.B. Etame, C.A. Smith, W.C.W. Chan, J.T. Rutka, Design and potential application of PEGylated gold nanoparticles with size-dependent permeation through brain microvasculature, nanomedicine: nanotechnology. Biol. Med. **7**, 992–1000 (2011)
15. M. Shakibaie, H. Forootanfar, K. Mollazadeh-Moghadam, Z. Bagherzadeh, N. Nafissi-Varcheh, A.R. Shahverdi, M.A. Faramarzi, Green synthesis of gold nanoparticles by the marine microalga *Tetraselmis suecica*. Biotechnol. Appl. Biochem. **57**, 71–75 (2010)
16. Y.L. Luo, Y.S. Shiao, Y.F. Huang, Release of photoactivatable drugs from plasmonic nanoparticles for targeted cancer therapy. ACS Nano **5**, 7796–7804 (2011)
17. M. Vinod, K.G. Gopchandran, Au, Ag and Au: Ag colloidal nanoparticles synthesized by pulsed laser ablation as SERS substrates. Prog. Nat. Sci.: Mater. Int. **24**, 569–578 (2014)
18. C. Toccafondi, S. Thorat, R. La Rocca, A. Scarpellini, M. Salerno, S. Dante, G. Das, Multifunctional substrates of thin porous alumina for cell biosensors. J. Mater. Sci.: Mater. Med. **25**, 2411–2420 (2014)
19. D. Huang, F. Liao, S. Molesa, D. Redinger, V. Subramanian, Plastic-compatible low resistance printable gold nanoparticle conductors for flexible electronics. J. Electrochem. Soc. **150**, 412–417 (2003)
20. D.T. Thompson, Using gold nanoparticles for catalysis. Nano Today **2**, 40–43 (2007)
21. F. Schulz, T. Homolka, N.G. Bastus, V. Puntes, H. Weller, T. Vossmeyer, Little adjustments significantly improve the turkevich synthesis of gold nanoparticles. Langmuir **30**, 10779–10784 (2014)
22. P.R. Teixeira, M.S.C. Santos, A.L.G. Silva, S.N. Báo, R.B. Azevedo, M.J.A. Sales, L.G. Paterno, Photochemically-assisted synthesis of non-toxic and biocompatible gold nanoparticles. Coll. Surf. B **148**, 317–323 (2016)
23. S. Singh, D.V.S. Jain, M.L. Singla, One step electrochemical synthesis of gold-nanoparticles–polypyrrole composite for application in catechin electrochemical biosensor. Anal. Methods **5**, 1024–1032 (2013)
24. R.A.B. Alvarez, M. Cortez-Valadez, L.O.N. Bueno, R.B. Hurtado, O. Rocha-Rocha, Y. Delgado-Beleño, C.E. Martinez-Nuñez, L.I. Serrano-Corrales, H. Arizpe-Chávez, M. Flores-Acosta, Vibrational properties of gold nanoparticles obtained by green synthesis. Physica E **84**, 191–195 (2016)
25. G. Compagnini, A. Scalisi, O. Puglisi, C. Spinella, Synthesis of gold colloids by laser ablation in thiol alkane solutions. J. Mater. Res. **19**, 2795–2798 (2004)
26. H. Zeng, X.W. Du, S.C. Singh, S.A. Kulinich, S. Yang, J. He, W. Cai, Nanomaterials via laser ablation/irradiation in liquid: a review. Adv. Funct. Mater. **22**, 1333–1353 (2012)
27. V. Amendola, M. Meneghetti, What controls the composition and the structure of nanomaterials generated by laser ablation in liquid solution? Phys. Chem. Chem. Phys. **15**, 3027–3046 (2013)
28. R.G. Nikov, A.S. Nikolov, N.N. Nedyalkov, P.A. Atanasov, M.T. Alexandrov, D.B. Karashanova, Processing condition influence on the characteristics of gold nanoparticles produced by pulsed laser ablation in liquids. Appl. Surf. Sci. **274**, 105–109 (2013)
29. A. Pyatenko, K. Shimokawa, M. Yamaguchi, O. Nishimura, M. Suzuki, Synthesis of silver nanoparticles by laser ablation in pure water. Appl. Phys. A **79**, 803–806 (2004)
30. R. Intartaglia, M. Rodio, M. Abdellatif, M. Prato, M. Salerno, Extensive characterization of oxide-coated colloidal gold nanoparticles synthesized by laser ablation in liquid. Materials **9**, 775 (2016)
31. G. Compagnini, A.A. Scalisi, O. Puglisi, Production of gold nanoparticles by laser ablation in liquid alkanes. J. Appl. Phys. **94**, 7874–7877 (2003)
32. V. Amendola, S. Polizzi, M. Meneghetti, Laser ablation synthesis of gold nanoparticles in organic solvents. J. Phys. Chem. B **110**, 7232–7237 (2006)
33. V. Amendola, S. Polizzi, M. Meneghetti, Laser ablation synthesis of silver nanoparticles embedded in graphitic carbon matrix. Sci. Adv. Mater. **4**, 497–500 (2012)
34. G. Compagnini, A.A. Scalisi, O. Puglisi, Ablation of noble metals in liquids: a method to obtain nanoparticles in a thin polymeric film. Phys. Chem. Chem. Phys. **4**, 2787–2791 (2002)
35. V. Amendola, G.A. Rizzi, S. Polizzi, M. Meneghetti, Synthesis of gold nanoparticles by laser ablation in toluene: quenching and recovery of the surface plasmon absorption. J. Phys. Chem. B **109**, 23125–23128 (2005)

36. T. Mortier, T. Verbiest, A. Persoons, Laser ablation of gold in chloroform solutions of cetyltrimethylammoniumbromide. Chem. Phys. Lett. **382**, 650–653 (2003)
37. V. Amendola, G. Mattei, C. Cusan, M. Prato, M. Meneghetti, Fullerene non-linear excited state absorption induced by gold nanoparticles light harvesting. Synth. Met. **155**, 283–286 (2005)
38. S.-P. Chen, H.-L. Chiu, P.-H. Wang, Y.-C. Liao, Inkjet printed conductive tracks for printed electronics. ECS J. Solid State Sci. Technol. **4**, 3026–3033 (2015)
39. M.J. Beliatis, S.J. Henley, S. Han, K. Gandhi, A.A.D.T. Adikaari, E. Stratakis, E. Kymakis, S.R.P. Silva, Organic solar cells with plasmonic layers formed by laser nanofabrication. Phys. Chem. Chem. Phys. **15**, 8237–8244 (2013)
40. J. Macicek, Adv. X-ray Anal. **35**, 687–691 (1992)
41. A.O. Simm, C.E. Banks, S.J. Wilkins, N.G. Karousos, J. Davis, R.G. Compton, A comparison of different types of gold–carbon composite electrode for detection of arsenic(III). Anal. Bioanal. Chem. **381**, 979–985 (2005)
42. H. Sakai, Surface-induced melting of small particles. Surf. Sci. **351**, 285–291 (1996)
43. A.S. Nikolov, R.G. Nikov, N.N. Nedyalkov, P.A. Atanasov, M.T. Alexandrov, D.B. Karashanova, Modification of the silver nanoparticles size-distribution by means of laser light irradiation of their water suspensions. Appl. Surf. Sci. **280**, 55–59 (2013)
44. J. Liao, Y. Zhang, W. Yu, L. Xu, C. Ge, J. Liu, N. Gu, Linear aggregation of gold nanoparticles in ethanol. Colloid. Surf. A **223**, 177–183 (2003)
45. P. Boyer, M. Meunier, Modeling solvent influence on growth mechanism of nanoparticles (Au, Co) synthesized by surfactant free laser processes. J. Phys. Chem. C **116**, 8014–8019 (2012)
46. G. Cristoforetti, E. Pitzalis, R. Spiniello, R. Ishak, F. Giammanco, M. Muniz-Miranda, S. Caporali, Physico-chemical properties of Pd nanoparticles produced by pulsed laser ablation in different organic solvents. Appl. Surf. Sci. **258**, 3289–3297 (2012)
47. E. Giorgetti, M. Muniz-Miranda, P. Marsili, D. Scarpellini, F. Giammanco, Stable gold nanoparticles obtained in pure acetone by laser ablation with different wavelengths. J. Nanopart. Res. **14**, 1–13 (2012)